

Critical Dynamic Viscosities in a Binary Mixture¹

Y. Izumi,² H. Sawano,^{2,3} H. Sato,^{2,4} Y. Miyake,²
R. Kono,⁵ and H. Yoshizaki⁵

Ultrasonic shear measurements were conducted on polystyrene-cyclohexane solutions at 3, 51, and 252 kHz using the crystal fork and torsion methods. The real and imaginary parts of the complex shear modulus above the critical point are compared with modified theoretical expressions derived within the framework of the decoupled-mode theory. For this comparison, a background part was assumed to be described by a scaling form proposed by de Gennes. Numerical analysis of the data shows a satisfactory agreement between the theory and the experiments for ultrasonic shear data over a wide range of reduced frequency ω^* . In addition, it is shown that the description of the simple viscosity dynamical scaling function is broken at a high-frequency limit.

KEY WORDS: critical phenomena; cyclohexane; polystyrene; shear modulus; ultrasonics; viscosity.

1. INTRODUCTION

In a previous paper [1], ultrasonic shear data along the critical isochore in xenon and in the binary mixture nitrobenzene-*n*-hexane were interpreted in terms of modified theoretical expressions derived within the framework of decoupled-mode theory. Although the numerical analysis of the data has shown a rather satisfactory agreement between the theory and the experiments for ultrasonic shear data, we did not claim that these tests are

¹ Paper presented at the Tenth Symposium on Thermophysical Properties, June 20–23, 1988, Gaithersburg, Maryland, U.S.A.

² Department of Polymer Science, Hokkaido University, Sapporo 060, Japan.

³ Present address: The Fujikura Cable Works Ltd., Sakura, Chiba 285, Japan.

⁴ Present address: Ibaraki Electrical Communication Laboratory, Nippon Telegraph and Telephone Public Corporation, Tokai, Ibaraki 319-11, Japan.

⁵ Department of Applied Physics, National Defense Academy, Yokosuka 239, Japan.

conclusive because of the scattering of our experimental data. Furthermore, we desired to improve the ultrasonic shear measurements and investigate the viscosity over a wide range of frequency in various binary systems in order to obtain more conclusive results. To improve the measurements we used a network analyzer system described later. By choosing a polymer solution as the binary mixture, we were able to test the theory over a wide range of reduced frequency ω^* , because the polymer solution is characterized by a high viscosity and a large correlation length in comparison with simple pure fluids and binary mixtures of low molecular weight.

In this paper, we report measurements on the ultrasonic shear viscosity for polystyrene in cyclohexane at the critical solution concentration in the one-phase region as a function of temperature and frequency. This system has been thoroughly examined over the past decade by coexistence-curve measurements [2], light-scattering measurements [2, 3], static shear viscosity measurements [4], and line-width measurements [5]. These data enabled us to test the theory of the dynamic viscosity over a wide range of ω^* . Experiments were conducted with a carefully fractionated polymer sample to minimize the effect of the molecular weight distribution.

2. EXPERIMENTAL

The fork and torsion crystal techniques described in previous papers [6-8] were used for dynamic viscosity measurements. The vibration of the crystal is damped by immersing it in a liquid to be measured, and the properties of liquid in shear may be calculated from the resulting changes in the resonant frequency Δf and in the resistance Δr corresponding to the resonant frequency on the motional admittance circle of the crystal, compared with the corresponding values in air. These quantities are related to the real and imaginary parts (R and X , respectively) of the shear mechanical impedance Z by the equations

$$Z = R + iX \quad (1)$$

$$R = \Delta r / 2 \sqrt{2} K \quad (2)$$

$$X = \Delta f / \sqrt{2} K \quad (3)$$

where K is a constant for a particular crystal and is determined from Newtonian liquids through the equation,

$$K = \Delta f / \sqrt{\rho_N \eta_N \omega} \quad (4)$$

where ρ_N and η_N are the density and the viscosity in Newtonian liquids,

respectively, and ω is the ultrasonic shear wave frequency. The crystal was connected electrically with a network analyzer [Hewlett Packard (HP) 3570A] through a VHF switch (HP 59307A). The network analyzer was used to measure the electrical impedance of the torsional crystal. For a frequency source a synthesizer (HP 3330B) was used. This HP 3042A network analyzer system is connected by the HP-IB interface bus and controlled by a computer (HP 9825A). The output is printed out and also made on a plotter (HP 9862A). The block diagram of this system is shown in Fig. 1.

Polystyrene ($M_w = 11 \times 10^4$ and $M_w/M_n < 1.02$, with M_w and M_n being the weight- and the number-average molecular weight, respectively) in cyclohexane was used in the present work. The sample preparation and critical mixing point ($T_c = 21.455^\circ\text{C}$, $\phi_c = 0.0825$ by volume fraction) have been fully described elsewhere [4].

The crystals of 3, 51, and 252 kHz were separately suspended in three 2-cm-diameter, 10-cm-long glass cells, which were sealed with mercury to avoid concentration changes. The change in concentration by evaporation during the course of the experiment was less than 0.006% in weight of cyclohexane. Each mixture was well stirred before and after it was poured into the ultrasonic cell, and rest periods of more than 30 min were allowed to ensure the establishment of equilibrium in the system before the measurements were made at each temperature. Above the critical temperature, it was found that there was no difference between stirring and not stirring the solution. This means that gravitational effects are probably not important. The ultrasonic cell was placed in a water Dewar vessel along with a thermostat which provided a constant temperature within 0.002 K. The temperature was measured by a quartz thermometer (HP 2801A). The values of static viscosity and density have been reported elsewhere [4].

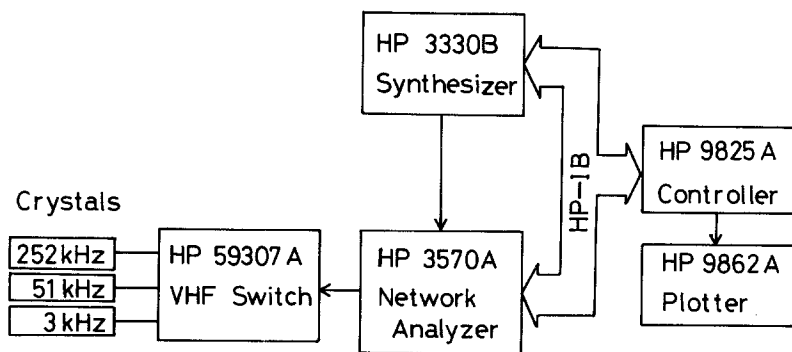


Fig. 1. Block diagram of the measuring system (HP 3042A network analyzer system).

3. DATA ANALYSIS

The complex viscosity η^* is separated into real and imaginary parts as follows:

$$\begin{aligned}\eta^* &= \eta' - i\eta'' \\ &= (\eta'_B + \Delta\eta') - i(\eta''_B + \Delta\eta'')\end{aligned}\quad (5)$$

The real and imaginary parts of the complex viscosity η^* are written by using the real and imaginary parts of the shear mechanical impedance as follows:

$$\eta' = 2XR/\omega\rho \quad \text{and} \quad \eta'' = (R^2 - X^2)/\omega\rho \quad (6)$$

where ρ is the density of critical solution.

The critical component $\Delta\eta^*$ ($\equiv \Delta\eta' - i\Delta\eta''$) is expressed in terms of the following theoretical expressions derived within the framework of the decoupled-mode theory [1, 10]:

$$\Delta\eta'(\omega, \kappa) = \frac{8}{15\pi^2} \bar{\eta}(\kappa) S_1 = \frac{8}{15\pi^2} \bar{\eta}(\kappa) \int_0^{q_c/\kappa} \frac{dv \cdot v^8}{(1+v^2)^{3/2} [v^4(1+v^2) + \omega^{*2}]}, \quad (7)$$

$$\Delta\eta''(\omega, \kappa) = \frac{8}{15\pi^2} \bar{\eta}(\kappa) S_2 = \frac{8}{15\pi^2} \bar{\eta}(\kappa) \int_0^{q_c/\kappa} \frac{dv \cdot v^6 \omega^*}{(1+v^2)^2 [v^4(1+v^2) + \omega^{*2}]}, \quad (8)$$

respectively, where $v = q/\kappa$, q is a wave vector, κ is the reciprocal correlation length, the reduced frequency $\omega^* = \omega/\omega_D$, the characteristic frequency $\omega_D = k_B T \kappa^3 / 8\bar{\eta}(\kappa)$, and the cutoff wave number q_c is a free parameter to be fixed by fitting the shear viscosity data to Eq. (9). In the limit of $\omega \rightarrow 0$, Eq. (7) is

$$\begin{aligned}\Delta\eta(\kappa) &= \frac{8}{15\pi^2} \bar{\eta}(\kappa) S_3 \\ &= \frac{8}{15\pi^2} \bar{\eta}(\kappa) \left\{ -\frac{q_c/\kappa}{(q_c^2/\kappa^2 + 1)^{1/2}} - \frac{(q_c/\kappa)^3}{3(q_c^2/\kappa^2 + 1)^{3/2}} \right. \\ &\quad \left. + \ln |q_c/\kappa| + (q_c^2/\kappa^2 + 1)^{1/2} \right\}\end{aligned}\quad (9)$$

The above-mentioned theory predicts only the critical part of the complex viscosity.

Next we evaluate the background component η_B^* ($\equiv \eta_B' - i\eta_B''$). In fluids and binary mixtures, η_B^* does not depend on ω in the range of ultrasonic shear wave frequency, while η_B^* in a polymer solution depends on ω drastically. This fact has complicated the data analysis of η_B^* in a polymer solution, as pointed out previously [17]. In the present paper, η_B' and η_B'' were evaluated by assuming the scaling forms proposed by de Gennes [11], because of the reasons described in the following section:

$$\begin{aligned} (\eta_B' - \eta_s)/(\eta_B - \eta_s) &= c_1'(\omega\tau)^{-c_2'} [1 + \dots] \\ \eta_B''/(\eta_B - \eta_s) &= c_1''(\omega\tau)^{-c_2''} [1 + \dots] \end{aligned} \quad (10)$$

Here c_1' , c_2' , c_1'' , and c_2'' are empirical constants determined by the data outside the region in which a simple power law is realized [4], η_B was previously estimated by the Vogel equation [4], η_s is the solvent viscosity, and τ is the relaxation time of a single chain which is estimated by the Rouse model and given by

$$\tau \equiv 6M(\eta_B - \eta_s)/\pi^2 cRT \quad (11)$$

where c is the concentration (g/cm^3) [12, 13].

In the static limit,

$$\lim_{\omega \rightarrow 0} \eta_B' = \eta_B \quad \text{and} \quad \lim_{\omega \rightarrow 0} \eta_B'' = 0 \quad (12)$$

Only the data at 51 and 252 kHz have been analyzed, because the accuracy of the data at 3 kHz is slightly less than that at other frequencies. The parameters which are required in a comparison of the data with the theory are the reciprocal correlation length κ and the decay rate Γ_q obtained by light scattering [3] and Rayleigh line-width measurements [5]. Noting that the theory in the current state cannot discriminate among η , $\bar{\eta}$, and η_B [14, 15], we regard $\bar{\eta}$ as η_B in the present analysis using Eqs. (7)–(9). In a more rigorous test of the theory, however, it is necessary to deduce $\bar{\eta}$ from line-width data, and then a more refined decoupled-mode equation should be compared with the results of viscosity measurements. The reciprocal correlation length κ and the cutoff parameter q_c are $1.72 \times 10^7 \varepsilon^{0.62} \text{cm}^{-1}$ [3] and $(2.17 \pm 0.04) \times 10^6 \text{cm}^{-1}$ [16], respectively, where ε is the reduced temperature difference.

4. RESULTS AND DISCUSSION

The results for the critical mixture are presented in Fig. 2. The solid line shows the Vogel equation, from which the static viscosity η deviates at

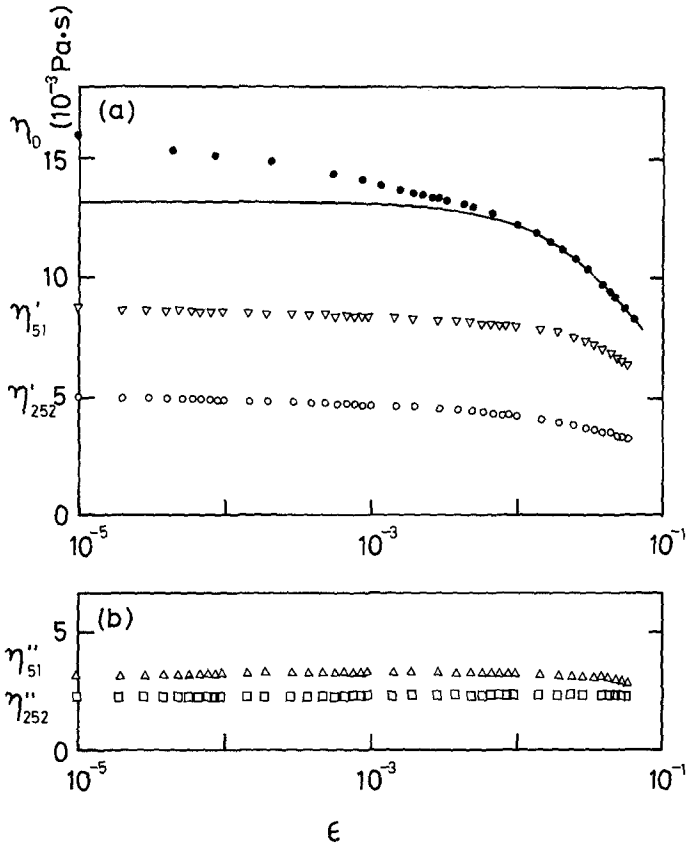


Fig. 2. Real part (a) and imaginary part (b) of the complex viscosity of polystyrene-cyclohexane as a function of the reduced temperature difference $\epsilon = (T - T_c)/T_c$. The solid line shows the background viscosity estimated from the Vogel equation.

about $\epsilon = 1.5 \times 10^{-2}$ [4]. It is clearly seen that η shows a divergence, while η' and η'' at 51 and 252 kHz show only slight divergences. The dynamic viscosity η' is less than the static shear viscosity η even in the range of the temperature outside the critical region. These behaviors of η' and η'' are almost explained by the viscoelastic properties of polymer solutions in the normal state. We have examined the following two models for η_B^* as a first step: the Rouse formula and the Doi formula [17]. It has been shown that the experimental data are expressed by the Rouse model rather than the Doi model. Further detailed examination based on the Rouse theory, however, showed that an essential refinement was able to be required in this theory for the quantitative agreement with the experiment. Any quan-

titative method for the refinement has not been presented as yet, although other evaluations of η_B^* have also been tried. As a result, the data points were analyzed by the scaling form described in Section 3. Noting that the present values of $\omega\tau$ are in the vicinity of $\omega\tau = 1$ [17], Eq. (10) cannot be applied in the original form. However, it was assumed that the scaling form of Eq. (10) was preserved, as long as the constants are regarded as the empirical constants: c'_1 , c'_2 , c''_1 , and c''_2 are 0.67, 0.45, 0.31, and 0.76 in the range of $0.86 < \omega\tau < 1.22$ for 51 kHz and 0.38, 0.14, 1.04, and 0.96 in the range of $4.42 < \omega\tau < 6.03$ for 252 kHz, respectively. Higher terms in Eq. (10) were introduced to take into account deviations from the main term, although the terms were not used in the present analysis.

The critical excess viscosities are thus determined and plotted against ϵ in Fig. 3, where the size of the error bars was determined by taking into account the standard deviation occurred in the curve fitting of the

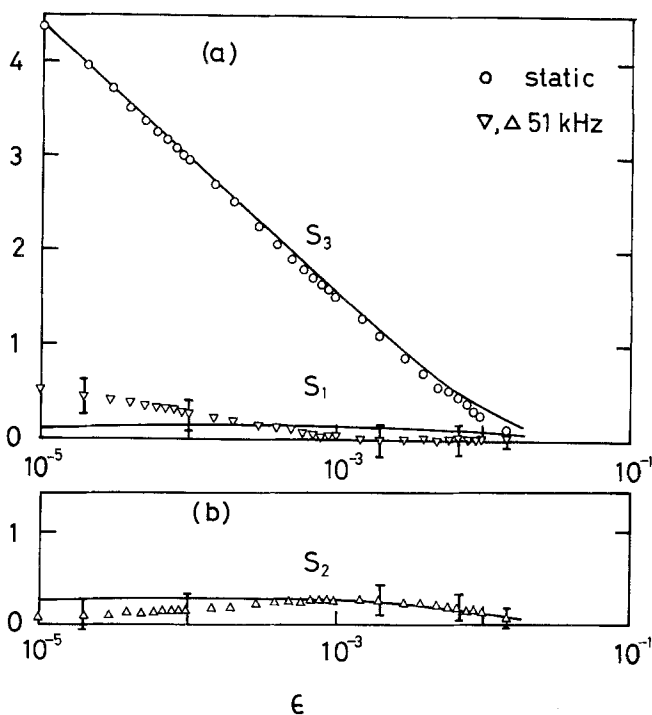


Fig. 3. Real part (a) and imaginary part (b) of the excess complex viscosity of polystyrene-cyclohexane as a function of the reduced temperature difference ϵ . (a) The solid lines show Eqs. (7) and (9), and (b) the solid line shows Eq. (8) corresponding to 51 kHz, respectively.

parameters of the Vogel equation and those in Eq. (10) [18]. The values of excess viscosities $\Delta\eta'$ and $\Delta\eta''$ at 252 kHz are very small. From Fig. 3, it can be easily understood that the dynamical viscosity in the polymer solution shows a significant frequency dependence at ultrasonic frequencies: $\Delta\eta'$ and $\Delta\eta''$ are almost zero. It is further noted that the behaviors of $\Delta\eta$, $\Delta\eta'$, and $\Delta\eta''$ are approximately expressed by Eqs. (7)–(9), as shown by the solid lines in Fig. 3.

To study the frequency dependence of the viscosity function, a normalized dynamical scaling function $\sigma_{\text{PF}}(\omega^*)$ has been introduced by subtraction of Eq. (7) from Eq. (9) for the static limit $\omega = 0$:

$$\frac{\Delta\eta(\kappa) - \Delta\eta'(\omega, \kappa)}{\bar{\eta}(\kappa)} = \frac{\eta(\kappa) - \eta'(\omega, \kappa)}{\bar{\eta}(\kappa)} = \frac{8}{15\pi^2} \sigma_{\text{PF}}(\omega^*) \quad (13)$$

In taking the difference within the integral sign, we previously obtained an integral which converged at the upper limit [1]: that is, the upper limit can be set equal to infinity, $q_c/\kappa \rightarrow \infty$. We call $\sigma_{\text{PF}}(\omega^*)$ the simple dynamical scaling function. However, because the upper limit in the integral cannot be regarded as infinity in the present experiment, the behavior at high frequencies is not expressed by the simple scaling function but by a more complex function,

$$\tilde{\sigma}_{\text{PF}}(q_c/\kappa, \omega^*) = \int_0^{q_c/\kappa} \frac{dv \cdot v^4 \omega^{*2}}{(1+v^2)^{5/2} [v^4(1+v^2) + \omega^{*2}]} \quad (14)$$

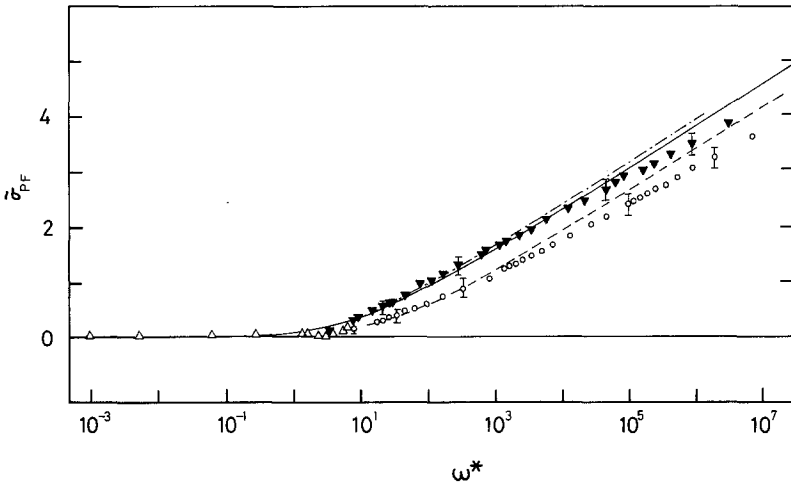


Fig. 4. Viscosity dynamic function $\tilde{\sigma}_{\text{PF}}(q_c/\kappa, \omega^*)$ as a function of reduced frequency ω^* . Ultrasonic shear data are shown at 38.7 kHz (Xe; open triangles), 51 kHz (filled inverted triangles), and 252 kHz (open circles) in polystyrene-cyclohexane. The dot-dashed, solid, and dashed curves represent Eq. (14) corresponding to 3, 51, and 252 kHz, respectively.

The normalized dynamical function $\tilde{\sigma}_{\text{PF}}(q_c/\kappa, \omega^*)$ is plotted against the reduced frequency ω^* in Fig. 4. The most interesting result is that the normalized dynamical function behaves quite similarly in one- and two-component systems except at high frequencies and that the dynamical data generally follow the prediction of the theory over a wide range of ω^* .

Thus the Perl–Ferrell theory may be successfully applied to explain the behavior of the dynamic viscosity. However, we do not claim that these tests are conclusive because of the introduction of the empirical constants. It is necessary to improve the method for the evaluation of η_B^* in order to obtain more conclusive results. Research is in progress along this line.

ACKNOWLEDGMENTS

Calculations were carried out on the HITAC M682H Computer of the Computer Center at Hokkaido University. This work was partly supported by a Grant-in-Aid from the Ministry of Education, Science and Culture.

REFERENCES

1. Y. Izumi, Y. Miyake, and R. Kono, *Phys. Rev.* **A23**:272 (1981).
2. J. Kojima, N. Kuwahara, and M. Kaneko, *J. Chem. Phys.* **63**:333 (1975).
3. N. Kuwahara, J. Kojima, and M. Kaneko, *Phys. Rev.* **A12**:2606 (1975).
4. Y. Izumi, H. Sawano, and Y. Miyake, *Phys. Rev.* **A29**:826 (1984).
5. Q. H. Lao, B. Chu, and N. Kuwahara, *J. Chem. Phys.* **62**:2039 (1975).
6. Y. Miyake, Y. Izumi, and R. Kono, *Phys. Rev.* **A15**:2065 (1977).
7. W. P. Mason, *Trans. Am. Soc. Mech. Eng.* **69**:359 (1947).
8. W. P. Mason, *Physical Acoustics and the Properties of Solid* (Van Nostrand, New York, 1958), pp. 54, 114.
9. K. Yamamoto, Y. Yamada, and Y. Wada, *Oyo Buturi* **27**:98 (1958).
10. R. Perl and R. A. Ferrell, *Phys. Rev. Lett.* **29**:51 (1972); *Phys. Rev.* **A6**:2358 (1972).
11. P.-G. de Gennes, *Scaling Concepts in Polymer Physics* (Cornell University, Ithaca, N.Y., and London, 1979), pp. 185–186.
12. P. E. Rouse, Jr., *J. Chem. Phys.* **21**:1272 (1953).
13. J. D. Ferry, *Viscoelastic Properties of Polymers* (John Wiley & Sons, New York, 1970), pp. 195–291.
14. J. V. Sengers, *AIP Conf. Proc.* **11**:229 (1973).
15. Y. Izumi and Y. Miyake, *Phys. Rev.* **A16**:2120 (1977).
16. Y. Izumi, H. Sawano, and Y. Miyake, *Rep. Prog. Polym. Phys. Jpn.* **25**:133 (1982).
17. Y. Izumi, Y. Miyake, R. Kono, and H. Yoshizaki, *Rep. Prog. Polym. Phys. Jpn.* **27**:77 (1984).
18. T. Nakagawa and Y. Oyanagi, in *Recent Developments in Statistical Inference and Data Analysis*, K. Matusita, ed. (North-Holland, Amsterdam, 1980), p. 221.